Preparing for JWST: a detailed simulation of a MOS deep field with NIRSpec

Giovanna Giardino, Pierre Ferruit, Jacopo Chevallard, Emma Curtis-Lake, Aurelien Jarno, Peter Jakobsen, Arlette Pecontal, Laure Piqeras, Nina Bonaventura and the JADES collaboration

ESA, ESTEC Keplerlaan 1 2200 AG Noordwijk - The Netherlands

E-mail: Giovanna.Giardino@esa.int

October 2018

Abstract.

JWST/NIRSpec will be the first multi-object spectrograph (MOS) to fly in space and it will enable the simultaneous measurement of up to $\sim$ 200 spectra over the wavelength range $\sim 0.6-5.3$ μm, allowing us to study the rest-frame optical properties of large samples of galaxies out to $z \sim 9$, and the rest-frame UV out to $z > 10$. This powerful instrument mode, however, requires careful planning of the observations and good understanding of the processing steps necessary to go from the detectors' count-rate images to background subtracted, calibrated spectra.

To support the community in preparing NIRSpec MOS programs and getting ready to analyze the data, we present here a set of simulations closely mimicking the deep spectroscopic observations that will be performed as part of the JADES survey, a joint effort of the NIRCam and NIRSpec GTO teams. The simulations are made possible by the NIRSpec Instrument Performance Simulator software, a Fourier Optics wave propagation module coupled with a detailed model of the instruments optical geometry and radiometric response, and a detector simulator reproducing the noise properties and response of NIRSpec's two H2RG sensors. The targets for the simulations were selected from the JWST Extragalactic Mock Catalog, JAGUAR (Williams et al. 2018).

The simulation data package delivered here include more than 60 count-rate images corresponding to the exposures break-down of the low and medium resolution part of one of the two NIRSpec deep-field spectroscopic programs of the JADES survey. The simulated data consists of three dither pointings, for 4 different instrument configurations (low and medium resolution over the entire NIRSpec wavelength range), plus the extracted, background subtracted, spectral traces for each of the 370 targets and corresponding 2D-rectified spectra and calibrated 1D spectra, as well as the mock astronomical data used as the simulation input.

1. Introduction

JWST is expected to revolutionize our view of galaxies at $z > 4$, and of low-mass galaxies at $1 < z < 4$, by providing powerful imaging and spectroscopic capabilities in the wavelength range $\lambda \sim 0.6 - 28$ μm. In particular, the Near Infrared Spectrograph,

NIRSpec [1, 2] on-board JWST will increase by more than an order of magnitude the emission line sensitivity in the wavelength region $\lambda \sim 1 - 2.5$ μm covered by existing ground-based instruments, while reaching an even greater sensitivity at wavelengths > 2.5 μm inaccessible with existing observatories. The multi-object spectroscopic (MOS) capabilities of NIRSpec will enable the simultaneous measurement of up to 200 galaxy spectra, allowing the observation of standard optical emission lines for large samples of galaxies out to $z \sim 9$ [3]

To be prepared to exploit NIRSpec MOS data as soon as they will be acquired once JWST begins its science operations, it is crucial to have a good understanding of their properties and idiosyncrasies. Chevallard et al.[3] have performed simulation of 1D, wavelength calibrated low-resolution NIRSpec spectra, of galaxies in the Hubble Ultra Deep Field (HUDF). They used the simulation of more than 700 spectra (constrained by photometric data from the Hubble eXtreme Deep Field – XDF) to assess the ability to derive different galaxy physical parameters, like star formation rates, ages, mass-to-light ratios, etc. for objects at redshift $z \sim 4 - 8$.

In this work we present simulations of a NIRSpec observation of a deep field, realistically reproducing the instrument data for a set of exposures, including nodding and dither patterns. We generate mock NIRSpec like data analogous to those that will be delivered by the standard processing at Level 1, 2 and 3. As template for the simulation we used one part of the NIRSpec Guaranteed Time Observation (GTO) program (see program GTO 1287‡). This program is part of the JWST Advanced Deep Extragalactic Survey (JADES), a joint project of the NIRCam and NIRSpec GTO teams and consists of a deep spectroscopic follow-up of high-redshift sources in GOODS-South area identified by deep imaging observations with NIRCam.

The deep-spectroscopy program consists of a 100 ks observation of a set of ~ 150 objects in instrument mode CLEAR/PRISM, that is spectral resolution ~ 100 over NIRSpec full wavelength range, plus $3\times$ 25 ks with instrument modes F070LP/G140M, F170LP/G235M, F290LP/G395M delivering medium resolution spectroscopy ($R \sim 1000$) over three NIRSpec bands (to cover the wavelength range $0.7 - 5.3$ μm) and 25 ks with instrument mode F290LP/G395H, $R \sim 3,000$ over the wavelength range $2.9 - 5.3 \mu m$.

We present here the simulated individual count-rate images for the prism and medium resolution gratings mode§. Together with the image files we also deliver the background subtracted traces, 2D rectified spectra and 1D-spectra, combined at nodding level. Although these products were generated with the GTO pipeline, the individual count-rate images have a format similar to that that will be produced by Level 1 of the official STScI pipeline. The processing steps of the official pipeline have been designed to closely match those of the GTO prototype.

The aim of this detailed simulation is to provide the astronomical community with a realistic NIRSpec data set from a MOS observations and offer insight into the various

‡ https://jwst.stsci.edu/observing-programs/program-information

§ simulations of the high resolution mode will follow

part of a MOS program and the corresponding data structure and format as well as a practical understanding of the peculiarities of such data and the necessary processing steps. This can inform the preparation of proposals and help to be ready to quickly exploit NIRSpec MOS data as soon as they become available.

The detailed simulations of the instrument response to the set of astronomical targets is made possible thanks to the Instrument Performance Simulator (IPS) software, a software tool that combines Fourier Optics computations, with a detailed geometrical description of the instrument and its radiometric response to generate maps of electron-rate per detector pixel, given the distribution of astronomical sources in NIRSpec field of view. The electron rate maps are then ingested in a detector simulator, that reproduce the detector response and noise properties, to generate count-rate images, closely resembling real exposures data from NIRSpec.

The key ingredient to build the astronomical scene for the simulation is a catalog of high-redshift galaxies with spectral information, from which the targets for the MOS observations can be selected. In this work, we used the JWST Extragalactic Mock Catalog generated by Williams et al.[4], using a novel phenomenological model for the evolution of galaxies and their properties, based on empirical constraints from current surveys between $0.2 < z < 10$. The model includes a self-consistent treatment of stellar and photoionized gas emission and dust attenuation based on the BEAGLE tool [5], so each source in the catalog has an associated spectral energy distribution, including emission lines. The targets for the simulations were selected using a software tool for MOS planning, developed by the JADES collaboration, that assign mini-slits to the sources in the field based on priority classes specified by the users and maximizing the number of targets observed in each pointing.

The paper is organized as follow in Sect. 2 we present the concept and main components of the IPS; in Sect. 3 the inputs mock astronomical data are described. The detail of the simulation steps, intermediate outputs and derived products are presented in Sect. 4.

2. The IPS and the detector simulator

The NIRSpec Instrument Performance Simulator (IPS) was developed alongside NIRSpec by the Centre de Recherche Astrophysique de Lyon (CRAL) as part of a contract with Airbus Defence and Space (the prime contractor for NIRSpec). It is implemented in `C++` with a Qt-based Graphical User Interface and runs on Linux systems. The software was initially developed to support the instrument design and assessment of performance-related trade-offs and for the early verification of the instrument performances [6, 7]. Subsequently, it has been used to provide simulated NIRSpec exposure to prepare the software tools necessary for the analysis of the data acquired during the instrument performance verification and calibration campaigns.

Currently the IPS is used for simulating data to support the GTO programs and the astronomical community, as in this case, and to support the testing and validation of the

NIRSpec data processing pipeline that is being developed at STScI. Indeed, the design of the IPS is such that the tool can be used for simulations of calibration exposures (that use test-equipment sources or the instrument internal calibration sources) as well as astronomical observations. The two main components of the IPS are a Fourier Optics wave-propagation module and a detector module reproducing the noise properties and response of NIRSpec's two H2RG sensors, used to go from the electron-rate maps generated by the Fourier Optics module to flight-like integration cubes. For the simulations delivered here however, we used a simpler detector simulator package implemented in Python, that uses electron-rate maps to generate count-rate maps, equivalent to NIRSpec Level 1 products as they will be delivered by the stage 1 'ramp-to-slopes' of STScI data-processing pipeline.

2.1. Fourier Optics module of the IPS

The philosophy behind this module is to be able to accurately follow the incoming light wavefront through the main optical planes of the instrument keeping into account the wavefront errors introduced by the different optical modules, the masking by the pupil and image-plane apertures, and the transmission efficiency of the individual elements. To do this the IPS contain a detailed geometrical and radiometric model of NIRSpec and the maps of wavefront errors, expressed in terms of Optical Path Differences (OPD), of all the main optical modules of the instrument and the Optical Telescope Element (OTE).

The geometrical model of the instrument is described in detail in Bernard et al.[8]. The authors show how dedicated calibration data from a small subset of NIRSpec modes and apertures can be used to optimize this parametric description of the instrument optical geometry to a high level of fidelity, that allows one to predict where a light ray entering NIRSpec will lend at the focal plane with an intrinsic accuracy better than a fraction of a pixel along the spatial and spectral direction. For the simulations set presented here we used the updated instrument parametric model derived by Giardino et al.[9] from calibration data acquired during the cryo-vacuum test campaign of the JWST Integrated Scientific Instrument Module (ISIM - CV3), that took place at NASA Goddard[10].

Fig. 1 in Bernard et al.[8] provides a schematic view of the Paraxial layout of the JWST telescope and NIRSpec optical train with the elements at the principal planes which are modeled within the Fourier Optics module of the IPS. In the case of a coherent light source, the propagation of the electromagnetic wavefront through NIRSpec's main optical planes is computed by Fourier transforming the electromagnetic complex field from one plane to the other, after having added the OPD from each optical module at the different propagation stages and applied the masking by the pupil and image-plane apertures. The Fourier transformations are implemented using the FFT algorithm.

This combined approach allows to accurately compute the shape and landing point of the point-spread function of a monochromatic point source at the focal plan and can

be easily extended to compute the spectral trace from a point source with continuum emission applying the same computation to a suitable wavelength grid. Concerning the amplitude of the PSF: slit and diffraction losses are caused by the aperture masking and folded into the wavefront propagation, while the throughput response of the various modules are applied as transmission coefficients. These coefficients are part of the radiometric model of the instrument and were derived from subsystem measurements when NIRSpec was being built. These are the same parameter values embedded in the signal-to-noise calculations for NIRSpec observations provided by JWST Exposure Time Calculator developed by Space Telescope Science Institute‖.

When dealing with the non-coherent light from extended sources the computation is broken down in three main steps. First, the illuminationin the MSA plane is computed by convolving the source intensity with the (pre-computed) PSF of the OTE and the instrument's fore optics, then the aperture masking at the MSA is applied, finally the signal at the focal plane is calculated by convolving the masked source with the spectrograph PSF.

Once the position, shape and amplitude of the PSF have been derived, the photon flux per pixel is converted into electron-rate maps using the (wavelength dependent) quantum efficiency maps of the two NIRSpec focal plane arrays¶. The two electron-rate maps for the two NIRSpec sensors is the output of this module and can be passed onto the next module to generate NIRSpec exposure files that include detector noise and detectors effects.

2.2. The detector simulator software

NIRSpec's focal plane is equipped with two 5.3 μm cutoff, Teledyne HAWAII-2RG sensor chip assemblies (SCAs), provided by NASA GSFC [11, 12]. We used a detector simulator implemented in Python to convert the (noiseless) electron-rate maps generated by the Fourier Optics module, into NIRSpec two count-rate files (one for each SCAs) as to mimic an exposure's count-rate maps generated by the ramp-to-slope processing pipeline from the raw integration cube. In the process, the simulation software folds onto the computation the shot noise of the sources' signal and the detector dark currents, readout noise, dark currents, detector gain, and optionally detector linearity effects, saturation, pixel-to-pixel cross talk due to Inter-Pixel Capacitance (IPC), as well as adding pixel 'cosmetic' defects such as hot-pixels, open pixels and pixels adjacent to open.

For a number of these detector effects, specifically the gain, readout noise, linearity/saturation response and dark currents, the software allows the user to select between (real) detector maps of these components or uniform averages applied across the arrays. In both cases, the maps or the scalar parameters used by the software are

‖ jwst.etc.stsci.edu

¶ The quantum efficiency maps are also part of the instrument radiometric model and also folded into the STScI ETC calculations

specific to each individual detectors and derived from the analysis of ground test data and they reflects the most up-to-date knowledge of the two H2RG sensors. Cosmetic defects are specified at the level of individual pixels using lists. Like the real NIRSpec detectors, the simulator requires the user to specify the readout mode. The options are grouped between 'Traditional' (modes: NRS and NRSRAPID) and 'IRS2' (modes: NRSIRS2 and NRSIRS2RAPID); within Traditional, the user can select to read out the full detector array or only a smaller subset ('window'-mode), while in IRS2 only the full-frame option is available – see [13] for more details. Once the mode is selected, the length of the exposure is determined by three parameters: the number of groups, the number of frames within each group, and the number of integrations.

Given these parameters, and dark currents and variance of the readout, the variance or total noise of an ideal, electronically shuttered instrument using multiaccum readout is given in Eq. 1 of Rauscher *et al.*[14, 15]. However, as shown by Birkmann et al.[16], the observed total noise in NIRSpec's dark exposures is somewhat higher than predicted for an ideal detector with the same read noise (as derived from CDS noise$^+$), because of the presence of a $1/f$-noise component in the readout electronics. A representative expression of the real detector noise is given by adding to the ideal formula an additional term of (excess) variance, as given by Eq. 3 and Eq. 4 of Birkmann et al.[16].

This empirical noise model is implemented in the detector package, with the value of the parameters (for dark currents, readout noise variance, etc.) as given in Table 2 of Birkmann et al.[16] and it is the one we used to generate the simulated NIRSpec count rate images for this program, from the simulated electron rate maps.

3. The Astronomical Scene

The target sources for the simulation were selected from the fiducial mock catalog of the JAdes extraGalactic Ultradeep Artificial Realizations (JAGUAR) package, developed by Williams et al.[4]. The catalog was generated using a novel phenomenological model for the evolution of galaxies and their properties, based on empirical constraints from current surveys between $0.2 < z < 10$. The model follows observed stellar mass functions, UV luminosity functions, integrated distributions including $M_{\rm UV}$-$M_\star$, β-$M_{\rm UV}$, and size-mass and size-$M_{\rm UV}$ distributions, and include galaxy SEDs thanks to self-consistent modeling of the stellar and nebular emission with the BEAGLE tool[5].

Like for the real NIRSpec MOS observations, sources have to be selected from the catalog and placed in the micro-apertures of NIRSpec Micro-Shutter Assembly (MSA), according to considerations of targets' priority and maximizing the use of the MSA multiplexing capability and detector area. For this purpose we used the eMPT tool developed by the GTO team[17] that optimizes the MSA fine pointing so as to capture spectra of as many of the highest priority targets as possible.

From the fiducial mock catalog extending on a 11×11-square FoV a subset covering

$^+$ where CDS stands for "Correlated Double Sampling" and means that the read-noise variance can be derived from from the variance of the difference of two adjacent groups in dark exposures

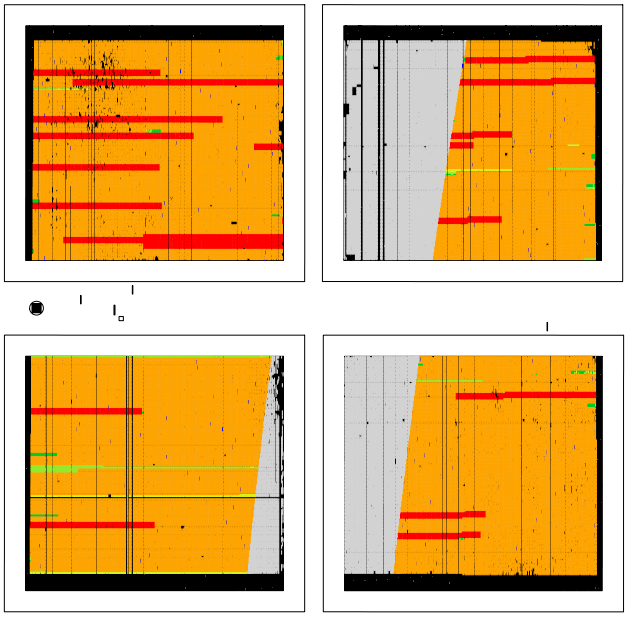

Figure 1. Source assignment to the MSA micro-shutters as determined by the eMPT tool for Dither 0. Orange indicate the MSA area used for the search. No source was placed in the gray area to avoid its spectrum to be affected by the detector gap. Green area are unused areas. Red areas could not be used due to the presence of defective shutters that cannot be closed and therefore would lead to the spectra of the targets to be contaminated. Black areas are shutters that are either defective and cannot be opened or deliberately kept closed to prevent electrical shorts in the MSA arrays. By zooming in the electronic version of the figure the individual slitlets that are being open for the (mock) observation are visible (in color blue).

a 3-arcmin radius circular FoV was derived containing 52,817 sources, sorted into 8 priority classes, plus fillers, as summarized in Table 1. The eMPT algorithm selected a total of 370 targets over the three dither pointing, where 23% (including by construction 9 Class 2 targets) are fully exposed and covered in all three dithers, 26% are 2/3-partially exposed and covered in two dithers and 51% are 1/3-exposed and only covered in one dither. Dither 1 and Dither 2 are located roughly -4 horizontal and $+2$ vertical shutters, and $+6$ horizontal and -7 vertical shutters from Dither 0. Fig. 1 displays the placing of the targets in the of MSA shutters for the case of Dither 0 (214 sources in this case).

The targets were selected by the eMPT algorithm to avoid overlapping of the sources' spectra in PRISM mode and truncation of the spectra caused by the gap between the two detectors in the NIRSpec focal plane. In the current baseline planning of the GTO program, the MOS configuration of the prism will be used to acquire the spectra of the same sources with the medium and high resolution gratings. This will lead to the sources' spectra overlapping over each other in these higher resolution modes. However the focus of the grating observation are the emission lines, which are

Table 1. Break-down of sources priority classes and corresponding numbers in input mock catalog and in selected targets (over three dithers)

Galaxy properties	Priority class	Mock catalog	Selected
place-holder	1	0	0
$z \geq 10$, $AB < 29.5$	2	17	9
$z \geq 10$, $29.5 < m_{\mathrm{F200W}} < 30.5$	3	31	4
$z > 6$, $\mathrm{S/N}_{H_\alpha} > 5$, $\mathrm{S/N}_{H_\beta} > 8$	4	100	7
$z > 2$, $\mathrm{S/N}_{\mathrm{continuum}} > 30$	5	139	13
$z > 6$, S/N < class 4	6	395	41
$1.5 < z < 6.5$, $27.25 < m_{\mathrm{F444W}} < 28.50$	7	4404	160
$m_{\mathrm{F444W}} <= 29$	8	14411	105
Filler	100	33319	31
Total N.		52817	370

rather sparse, while the continuum will be a weaker signal at the grating resolution, compared with the prism. So the strategy is to derive the source continuum from the prism observations, together with the strongest lines, and then use this information to disentangle the overlapping grating spectra. This approach is considered a reasonable tradeoff to achieve the same multiplexing level with the gratings as with the prism. Therefore, also for these simulations the same MOS configurations used for the PRISM over the three dithers was used for the simulation of the gratings mode. For this simulation, all the galaxies are modeled as point-sources.

To mimic real near-IR observations, the astronomical scene of the simulations has to include also the background emission. The background of a typical JWST observation will be comprised by the zodiacal light, the parasitic galactic emission, the parasitic zodiacal light and the thermal emission of the telescope. For this simulation, we have modeled the zodiacal light spectrum with the superposition of the a reddened spectrum of a solar analog and black-body spectrum for a temperature of 256.15 K. The solar-like spectrum is a synthetic spectrum generated by the Phoenix code for an effective temperature of 5800 K and solar gravity and metallicity. The reddening function is the one used by G. Aldering[18] (see also Leinert et al. [19]). For the normalization of the resulting spectrum, we have used the 1.25 micron value given in Giavalisco et al.[20] (and corresponding to 5.37 10^{-12} $\mathrm{Wm^{-2}m^{-1}}$).

In addition to the in-field zodiacal light component, JWST observations will also include a significant parasitic contribution of stray light, mainly due to the fact that JWST has an open telescope design. Wei and Lightsey[21] provides the results of detailed computations of this contributions for different sky locations and for different mirror cleanliness levels. The authors include two stray light components, the galactic sky and a component corresponding to the zodiacal light and the emission of the OTE, and provide computed values for a small set of wavelengths. For modeling the galactic sky light component we used a degree-3 polynomial fit to the values provided in Table 1 of Wei and Lightsey[21]. For the second component, we used the zodiacal light spectrum

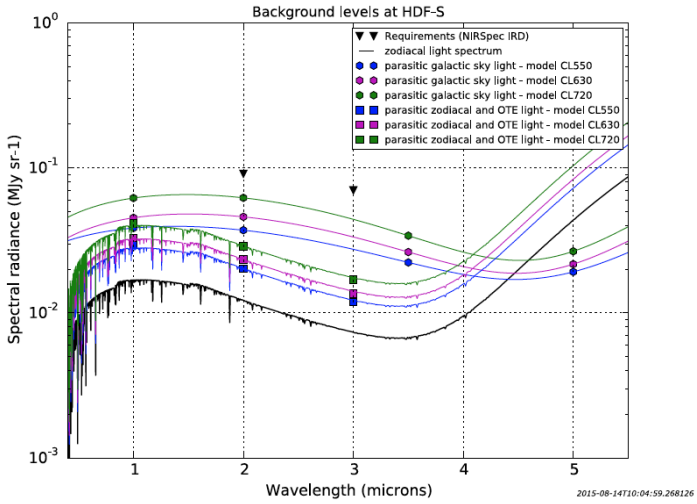

Figure 2. Spectra of the background components at the HDF-S location. We have modeled the zodiacal light spectrum as a superposition of a reddened spectrum of a solar analogue and a black-body spectrum ($T = 256.15$ K). The level of stray light is a function of the mirror cleanliness levels; in the simulations we adopted CL630.

normalized to the 2-micron values in their Table 2, since we expect that in our near-infrared wavelength range the dominant contributor will be stray light from the zodiacal light and not emission by the OTE.

The spectra of all the components contributing to the background signal in our simulations are shown in Fig. 2. For the parasitic components, as the amount of stray light is a function of the mirror cleanliness level, three different levels, identified here by CL550, CL630, CL720 are given. In our simulations we picked the intermediate CL630 level.

4. Simulated data and derived products

The astronomical scenes for the three dither and nodding positions provide the input for the IPS runs performed to generate the corresponding nine electron-rate images for each of the four instrument (disperser) configurations. These were combined with the corresponding electron-rate maps for the three background scenes generated for the three MOS-masks of the dithers and used as input to the detector module of the IPS to generate the count-rate maps for all the exposures planned in the GTO proposals and summarized in Table 2.

The same break-down of individual exposure of the GTO program was followed for the simulations and corresponding individual mock count-rate images have been generated for each exposure with Gaussian noise with STD (for signals and dark currents) given by Eq. 3 of Birkmann et al.[16] for 19 groups, divided by $\sqrt{2}$, given the 2 integrations for each exposure. This sums up to a total of 36 exposures in CLEAR/PRISM, for a total integration time of 100,838 s, and 9 exposures in each

Table 2. Break-down of GTO program 1287 and of the simulation presented here, in terms of instrument filter/disperser configurations, number of dithers, number of nodding per dither, and number of exposures per nodding positions. The integration time of each exposure is 2801 s.

Config.	n. dither	n. nodding	n. exposures	total n. exposures	total int. time
CLEAR/PRISM	3	3	4	36	100,838
G140M/F070LP	3	3	1	9	25,210
G235M/F170LP	3	3	1	9	25,210
G395M/F290LP	3	3	1	9	25,210
G395H/F290LP*	3	3	1	9	25,210

*Simulations of this mode are not included in this data set.

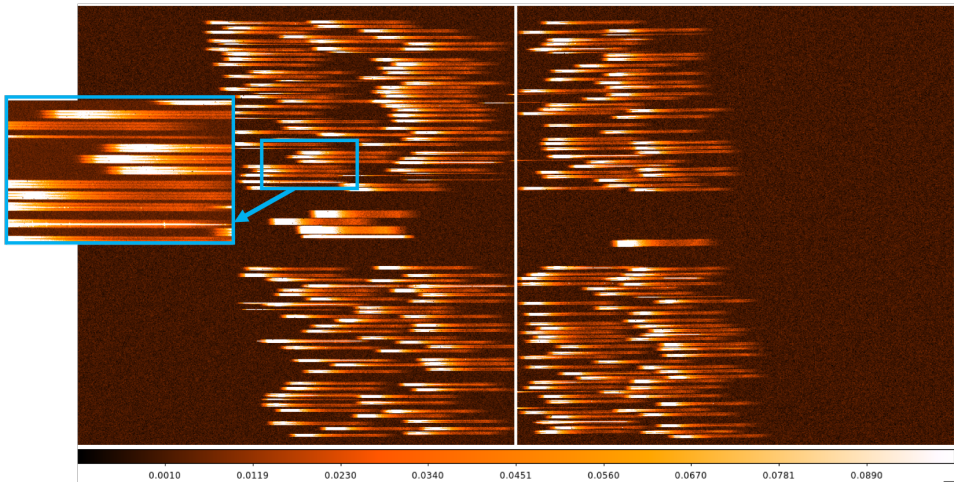

Figure 3. Count-rate image for one of the simulated prism exposure (for dither 0 and nodding 0). There are 214 targets packed in this MOS configuration, each one observed within a 3×1 slitlet. The noise level corresponds to that of an individual exposures of 2801 s. The inset provide a zoom-in on some of trace:, the spectra of a couple of stronger sources are visible above the background, as well as the spurious signal from one of the defective stuck-open shutters.

grating mode (25,210 s integration time), given that each exposure integration lasts 2801 s. Of the detector effects available in the detector simulator (see Sect 2.2, these simulated count-rate images only include the additional noise from subtracted dark currents and pixels correlations due to IPC. The count-rate image for one of the prism exposures is shown in Fig. 3 and that for one of the grating G235M exposures is shown in Fig. 4. As discussed in Sect. 3, the same MSA configuration was used to acquire the target spectra in the prism mode and the medium resolution gratings, resulting in the grating spectra overlapping with each other, as can be seen comparing the figures. The spectra of 214 (mock) galaxies is being observed in these exposures.

At this stage, default data processing would entail extracting the traces (i.e. spectra in wavelength-assigned detector-pixel space) of all sources from each individual (flat-fielded) exposures and then re-sampling and co-adding the traces of each sources from

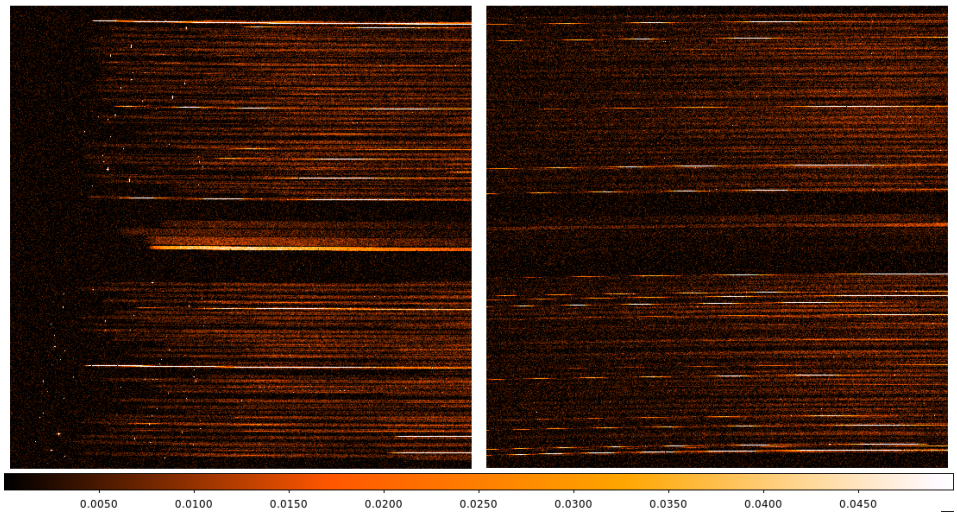

Figure 4. Count-rate image for one of the simulated exposure for grating G235M (dither 0 and nodding 0). The same MSA mask of open shutters as for the prism was used, corresponding to 214 targets. The noise level corresponds to that of an individual exposures of 2801 s

all exposures (where the source has been observed), to derive wavelength regularly-sampled 2D- or 1D-spectra with the total integration time for each target. However, nor the current version of the ESA Instrument Team's pipeline (NIPS) not that of the STScI pipeline (which is based on the Instrument Team's one) support traces from different paintings to be combined, yet. To by-pass this problem in the current deliver of the extracted products, using the detector software package, we have also generated exposures from the combined targets and background electron-rate maps for each nodding positions, with the exposure times corresponding to that of combining all exposures at a dither pointing, i.e. 33,612 s, for the prism, and 8403 s, for the gratings. From these we performed the background subtraction, by combing the three-nodding exposures, obtaining background-subtracted count-rate images for each dither points.

These images were flat-fielded (using simulated noiseless exposures of an ideal flat source) and processed with our extraction pipeline to generate, for each target, its spectral trace, the rectified 2D spectrum and the final 1D regularly sampled spectrum. NIPS uses the parametric model to locate the spectrum trace for a given slit, extract it as a sub-image, and then assign wavelength and spatial coordinates to each pixel in the sub-image according to the combination of slit, filter, and grating – see Appendix of Bernhard et.[8] for detailed description. The spectral trace is then re-sampled onto a regular grid of wavelength and spatial coordinates to produce the 2D-rectified image of the spectrum, from which the 1D regularly sampled spectrum can be derived by integrating the signal in the spatial direction ("collapsing").

The trace extracted from the simulations of the prism mode, for one of the targets (from the JAGUAR) catalog, a galaxy at $z = 7.3$, with $M = 6.5\ 10^8 M_\odot$ and UV luminosity $\sim 4.6\ 10^{28}$ ergs^{-1} is shown in Fig. 5. Note from the top-panel image of

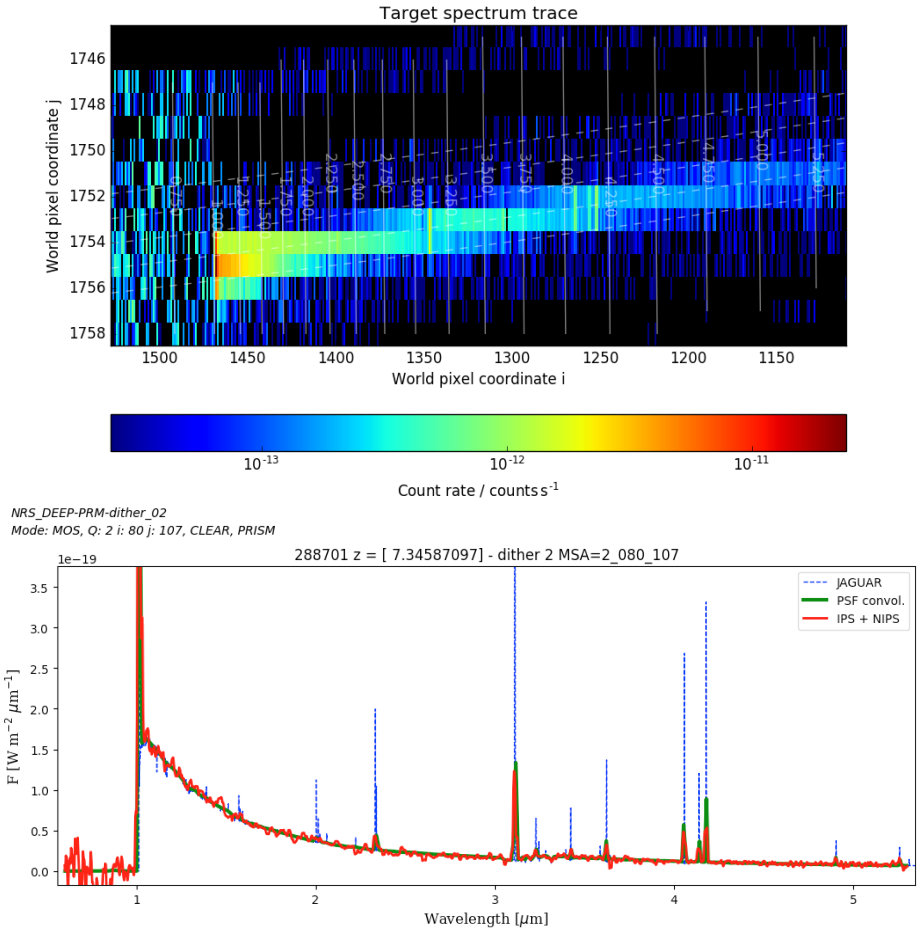

Figure 5. *Top panel* – Image of the spectral trace extracted from the simulated images for the prism mode for one of the target, a galaxy at $z = 7.3$, with $M = 6.5\ 10^8 M_\odot$ and UV luminosity $\sim 4.6\ 10^{28}$ergs^{-1}. Dashed lines indicate the slit center. *Bottom Panel* – Extracted final spectrum in red. The blue line indicate the simulation input spectrum from JAGUAR/BEAGLE and the green line the expected profile from binning the input spectrum at the the detector sampling. The simulation noise is equivalent to the ideal noise performance of 33,612 s exposure. Note that when binning the emission lines can have higher amplitude because (for a point source) all the line-flux falls on one pixel.

the trace data that the source is off-center within the slit; because in NIRSpec the MOS mode is implemented via the MSA array, the source positioning within the slit cannot be tightly controlled (unless one is prepared to pay a price in terms of reduced multiplexing). In the lower panel the extracted 1D-spectrum is compared to the input JAGUAR/BEAGLE spectrum and the convolution of this one with the instrument response. Note the high S/N of optical emission lines such as [OII]$_{\lambda 3729}$, [OIII]$_{\lambda 5007}$, H$_{\beta,\lambda 4861}$ and H$_{\gamma,\lambda 4340}$.

5. Data download and future plans

All the data presented here are publicly available and can be downloaded from ESA web site:

`www.cosmos.esa.int/jwst-nirspec-simulations`

This first release of simulated data based on the JADES program clearly include some drastic simplifications, for instance all sources are assumed to be point-like or the exclusion of cosmetic defects from the detector model, to name only the most significant. In addition, as mentioned above, the current limitations in the processing pipeline do not allow us to deliver high S/N spectra extracted from the simulated exposures directly. Moving forward, we plan to improve our simulation efforts and deliver ever better simulated data and products. Ultimately the data format of the simulated count-rate images will be made compatible for processing with the STScI official pipeline. Additionally we will also refine the data extraction and analysis process and describe the comparison between the input mock data and the one derived from NIRSpec in a future work.

To be kept up-to-date on new releases of NIRSpec simulated data you can register at:

`www.cosmos.esa.int/web/jwst-nirspec-simulations/register`

References

[1] Bagnasco G, Kolm M, Ferruit P *et al.* 2007 Overview of the near-infrared spectrograph (NIRSpec) instrument on-board the James Webb Space Telescope (JWST) *Cryogenic Optical Systems and Instruments XII* (*Society of Photo-Optical Instrumentation Engineers (SPIE) Conference Series* vol 6692) p 66920M

[2] Birkmann S M, Ferruit P, Rawle T *et al.* 2016 The JWST/NIRSpec instrument: update on status and performances *Space Telescopes and Instrumentation 2016: Optical, Infrared, and Millimeter Wave* (*Society of Photo-Optical Instrumentation Engineers (SPIE) Conference Series* vol 9904) p 99040B

[3] Chevallard J, Curtis-Lake E, Charlot S *et al.* 2017 *Submitted to MNRAS, ArXiv e-prints* (*Preprint* `1711.07481`)

[4] Williams C C, Curtis-Lake E, Hainline K N *et al.* 2018 *Accepted for publication in ApJS, ArXiv e-prints* (*Preprint* `1802.05272`)

[5] Chevallard J and Charlot S 2016 *MNRAS* **462** 1415–1443 (*Preprint* `1603.03037`)

[6] Piquéras L, Legay P, Legros E, Ferruit P, Pécontal A, Gnata X and Mosner P 2008 The JWST/NIRSpec instrument performance simulator *Society of Photo-Optical Instrumentation Engineers (SPIE) Conference Series* vol 7017

[7] Piquéras L, Legros E, Pons A, Legay P, Ferruit P, Dorner B, Pécontal A, Gnata X and Mosner P 2010 The JWST/NIRSpec instrument performance simulator software *Society of Photo-Optical Instrumentation Engineers (SPIE) Conference Series* vol 7738

[8] Dorner B, Giardino G, Ferruit P *et al.* 2016 *A&A* **592** A113

[9] Giardino G, Luetzgendorf N, Ferruit P *et al.* 2016 The spectral calibration of JWST/NIRSpec: results from the recent cryo-vacuum campaign (ISIM-CV3) *Space Telescopes and Instrumentation 2016: Optical, Infrared, and Millimeter Wave* (*Society of Photo-Optical Instrumentation Engineers (SPIE) Conference Series* vol 9904) p 990445

[10] Kimble R A, Vila M B, Van Campen J M *et al.* 2016 Cryo-vacuum testing of the JWST integrated science instrument module (ISIM) *Space Telescopes and Instrumentation 2016: Optical, Infrared, and Millimeter Wave* (*Society of Photo-Optical Instrumentation Engineers (SPIE) Conference Series* vol This conference)

[11] Rauscher B J, Alexander D, Brambora C K *et al.* 2008 James Webb Space Telescope Near-Infrared Spectrograph: dark performance of the first flight candidate detector arrays (*Society of Photo-Optical Instrumentation Engineers (SPIE) Conference Series* vol 7021)

[12] Rauscher B J, Boehm N, Cagiano S *et al.* 2014 *PASP* **126** 739–749

[13] Space Telescope Science Institute (STScI) 2016- NIRSpec Detector Readout Modes and Patterns JWST User Documentation updated 2017 April 19, Baltimore, USA https://jwst-docs.stsci.edu

[14] Rauscher B J, Fox O, Ferruit P *et al.* 2007 *PASP* **119** 768–786 (*Preprint* `0706.2344`)

[15] Rauscher B J, Fox O, Ferruit P *et al.* 2010 *PASP* **122** 1254 (Erratum)

[16] Birkmann S M, , Rawle T, Ferruit P *et al.* 2018 Noise Performance of the JWST/NIRSpec Detector System *Space Telescopes and Instrumentation 2018: Optical, Infrared, and Millimeter Wave* Society of Photo-Optical Instrumentation Engineers (SPIE) Conference Series p 99040B

[17] Jakobsen P, Bonaventura N, Ferruit P *et al.* 2018 *in preparation*

[18] Aldering, G 2001 SNAP Sky Background at the North Ecliptic Pole JWST User Documentation LBNL-51157 Lawrence Berkeley National Laboratory

[19] Leinert C, Bowyer S, Haikala L K *et al.* 1998 *Astronomy and Astrophysics Supplement Series* **127** 1–99

[20] Giavalisco M, Sahu K and Bohlin R C 2002 New Estimates of the Sky Background for the HST Exposure Time Calculator Tech. rep.

[21] Wei Z and Lightsey P A 2006 Stray light from galactic sky and zodiacal light for JWST *Society of Photo-Optical Instrumentation Engineers (SPIE) Conference Series* vol 6265 p 62653C